Comparison of breakup models for the secondary breakup in gas atomization

van Esch, Stijn J.A.

Award date:
2022

EINDHOVEN UNIVERSITY OF TECHNOLOGY

Department of Mechanical Engineering

Comparison of breakup models for the secondary breakup in gas atomization

BEP Report

S.J.A. van Esch (1462911)
Power & Flow

Supervisors:
dr. G. Finotello
D. Thuy

Eindhoven, 21 June 2022

Abstract

This thesis contributes to the phd project of the supervisor D. Thuy, who is investigating and modelling the whole gas atomisation. Gas atomisation is the process where a liquid flow gets disrupted by a high velocity gas stream. This disruption leads to a breakup of the liquid. There is known that the breakup can be described in two stages, the primary and secondary breakup. The focus in this thesis is only on the secondary breakup, where mainly is dealt with small droplets. A theoretical research is performed on models that describe the secondary breakup. From this research the TAB -and KH model have been chosen and are applied to simulations in the CFD software, openFoam. Liu et al. used the TAB and KH model for simulating secondary breakup in Benz applications as well. Their setup has been recreated in openFoam and the results are evaluated. Both models succeed in tracking the reference data from the paper. It turns out that the KH-model is more accurate as it aligns better with the experimental data. For future work, the models can be extended with turbulence models and the results should be evaluated. Also, a more in depth look in the effects of using molten metal should be performed such as the solidification.

Contents

1 Introduction

Additive manufacturing is becoming more and more popular as many companies are making their transition towards industry 4.0. This allows the shaping of complex and yet highly customizable parts which are able to meet any client's wishes. For the printing of metal parts, fine powder with a controlled size distribution is necessary to create quality end products. Also, the need for sustainability is inevitable and therefore the parts that are considered as scrap or have served their usage need to be reused. This allows more efficient material use. The material that will be recycled ought to be converted into fine powder. One way of obtaining fine powder from metal can be realized through the gas atomization process. Gas atomization in general is the process where a liquid flow is disrupted by a gas flow [1]. The first step in the atomization process, is melting the metal parts. Subsequently, the metal will be ejected from a nozzle as a stream of molten metal. In case a gas flow at high speed is exerted near the nozzle, a breakup flow is the result from this process. The interference between relatively the high velocity gas stream and low velocity liquid stream causes sinusoidal disturbances on the surface of the melt and is broken up in unstable liquid bodies, which are called ligaments [1]. The destabilization of the molten metal takes places in the primary atomization. The primary breakup can be seen in the light region closest to the melt tube in Figure 1.1. This destabilization is caused by turbulence and aerodynamic forces [2].

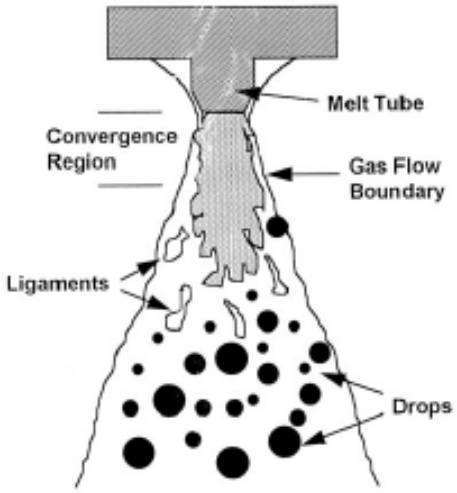

Figure 1.1: Schematic view of the gas atomisation process. [1]

The ligaments resulting from the primary breakup move further downstream and disintegrate into smaller droplets. Aerodynamic forces overcome the surface tension of the droplets, which causes the droplets to breakup into smaller droplets. The breakup stops until the surface tension is able to withstand the aerodynamic forces, which means that a stable droplet is formed. The droplets start to solidify into particles and the result is a fine powder.

In this thesis, the modelling of the secondary breakup is the main focus. The result of this paper will be of aid for the phd project of my supervisor Dennis. Dennis will be able to select an appropriate model for the secondary breakup and connect it to the whole modelling of the gas atomization. First a literature research is performed to form a theoretical basis of the secondary breakup and appropriate models that are able to describe the breakup. With the results and found methods the secondary breakup is modelled in the software OpenFoam. The results of the found models are validated with the results from the theoretical research. In the end, a recommendation on which breakup model results in the most accurate and reliable results is given.

2 Nomenclature

Symbol	**Meaning**	**Unit**	**Abbreviation**
a	Distorted droplet radius	meter	m
d	Damping constant	kilogram per second	kg/s
$D_{droplet}$	Droplet diameter	meter	m
m	Mass	kilogram	kg
k	Spring constant	Newton per meter	N/m
r_0	Initial droplet radius	meter	m
r	Current droplet radius	meter	m
U	Relative velocity	meter per second	m/s
η_{liquid}	Liquid dynamic viscosity	Pascal second	$Pa.s$
ρ_{gas}	Gas density	kilogram per cubic meter	kg/m^3
ρ_{liquid}	Liquid density	kilogram per cubic meter	kg/m^3
σ	Surface tension coefficient	kilogram per square second	kg/s^2

3 Theory

3.1 Introduction

The used models in the software openFoam are physical models that describe the breakup of droplets into smaller particles. As the goal for this thesis is to model the breakup in the CFD software a research of different models needs to be performed first. Two models, the Taylor Analogy Breakup and the Kelvin-Helmholtz theories are investigated and described in this chapter.

However, first important parameters that play a significant role in the models are explained in the next section.

3.2 Parameters

In describing the breakup, there are several key parameters. These parameters describe a significant part of the breakup. By only using these parameters predictions can already be made on the breakup mode or the behaviour of the flow. Also, the influence of the aerodynamic influence, inertia of the droplet and surface tension can be derived from these parameters.

The Weber number is one of the most important parameters in the description of the breakup. This is because the Weber number is a dimensionless number and represents the ratio between the fluid's inertial forces and its surface tension. Here the surface tension should be seen as the restoring force that wants to keep the droplet together. The deforming inertia forces are one of the forces that cause the droplet to breakup if they overcome the surface tension. The larger the Weber number gets, the larger the inertial forces become in comparison to the surface tension. A larger Weber number means in turn that the breakup will occur more chaotic. This can already be seen in Figure 3.1, where the breakup modes are visualized and ordered with an increase in the Weber number.

$$We = \frac{\rho_{gas} D_{droplet} U^2}{\sigma} \tag{3.1}$$

An additional parameter is the Ohnesorge number. As described in the introduction, the aerodynamic forces on the droplet play also a role in the deformation of the droplet surface. The surface tension counteracts the aerodynamic forces and keeps the droplet together. The viscosity of a liquid gives an indication of the amount of energy that can be dissipated from the aerodynamic forces. The latter is described in the Ohnesorge number [3]. A high Ohnesorge number indicates a lower likelihood of droplet breakup, because the influence of the viscosity increases with an increase in Ohnesorge number, which means more energy can be dissipated.

$$Oh = \frac{\eta_l}{\sqrt{\rho_l D_{droplet} \sigma}} \tag{3.2}$$

The Reynolds number is also an important parameter when it comes to describing flows in general. It is a dimensionless number just as the Weber and Ohnesorge number. The Reynolds number is the ratio of the inertia and viscous forces of the droplets. When the Reynolds number increases the influence of the droplets inertia becomes larger and the viscous forces lower. This means that the total amount energy being dissipated by the viscosity becomes less significant and therefore the breakup will become more dependent on the Weber number than the Ohnesorge and Reynolds number.

$$Re = \frac{\rho_{droplet} D_{droplet} U}{\eta_{droplet}} \tag{3.3}$$

In general, the flow in gas atomization is turbulent, the Reynolds number is large and the Ohnesorge number small. Therefore, the viscosity does not have a huge effect on dissipating the energy from the aerodynamic forces. There are fluids that have a high viscosity, for these fluids the Ohnesorge number becomes larger and thus the amount of energy that can be dissipated increases as well. This is a relation that describes and links the three parameters mentioned before and shows the coherency between them. Therefore, these three parameters are the key parameters for the secondary breakup.

Now there is a main understanding of the important parameters that help describing the physical behaviour of the breakup flow. In the next section different kinds of breakup modes are explained in more detail.

3.3 Breakup Modes

As aforementioned, there are various kinds of breakup modes. A breakup mode is the way of a droplet/ligament breaking up. The breakup is often a clearly recognizable and distinctive way. It is known that for a distinctive range of Weber numbers a certain type of breakup mode is present. This is because the fact that the viscosity of the molten metal is of less significance when it comes to dissipating the forces. Whereas the surface tension plays a larger role in this dissipation. Experiments performed by other researches have shown that the transition between two modes is a continuous process. However, for the sake of simplicity it is often assumed to occur abruptly [4]. The transition turns out to be a strong function of the Weber number and less dependent on the Ohnesorge number and Reynolds number [4]. The various breakup modes are visualized in Figure 3.1.

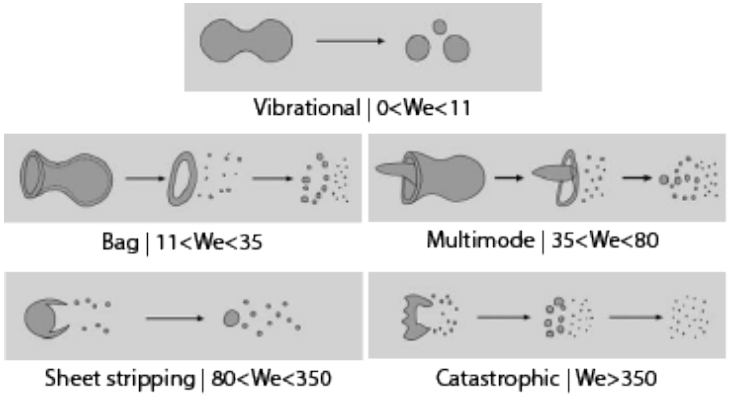

Figure 3.1: Different breakup modes dependent on the Weber number. [4]

3.3.1 Vibrational

The occurrence of vibrational breakup is rather low compared to the ones to follow, this is because the vibrational breakup does not lead to small fragment sizes in the end of the breakup and therefore not desired when gas atomization is used. The vibrational breakup is caused by oscillations at the natural frequency of the droplet [4]. The fragments resulting from this type of breakup are still relatively large and comparable to the size of the parental droplet.

3.3.2 Bag Breakup

If the Weber number comes in the range of 11<We<35 the so called bag breakup occurs. This breakup can be divided into four stages. These four stages are the deformation, bag growth, bag breakup and ring breakup. In essence, the bag breakup can be described as a droplet/ligament deforming into the shape of a bag. This bag gets disrupted and a ring will result from the bag

breakup. Eventually, this torus breaks up as well and smaller droplets are the result. The bag breakup is visualized in subfigure (b) of Figure 3.1.

3.3.3 Multimode

As mentioned before, the type of change between breakup modes is a continuous process. The multimode breakup can be seen as a phase between the bag breakup and sheet thinning. The multimode can be described by using two stages, which are called bag-plume breakup and plume-shear breakup [5], visible in subfigure (c) of Figure 3.1. The plume can be seen [5] as the liquid stream inside the bag.

3.3.4 Sheet thinning

Sheet thinning occurs at larger velocities than the vibrational, bag breakup or multimode breakups. In sheet thinning ligaments get disrupted from the periphery of the parent droplet. After the disruption the fragment breaks up in multiple fragments. This is a continuous process until the parent droplet is completely disrupted.

3.3.5 Catastrophic

Catastrophic breakup is the type of breakup that occurs at large velocities. However, the drop sizes and velocities involved in these type of sprays are not often in the range of the values for the catastrophic breakup to occur. In the catastrophic breakup the unstable surface waves that are growing on the droplet surfaces are increasing in such a fast manner that the disruptive waves penetrates the drop and causes it to breakup, before it is possible to form a bag or to allow sheet stripping.

The aforementioned breakup modes give a slight indication on the result of such a breakup. As the breakup modes are a strong function of the Weber number, an indication of the drop sizes can be known if the Weber number is known. A larger Weber number results for the breakup modes in a more chaotic one. The more chaotic the breakup mode, the smaller the droplets become. Therefore, it is appropriate to know in which breakup mode an experiment or simulation will be. In this thesis this is mainly the bag and sheet stripping mode, which is also observed in Table 5.1 presented by Liu et al. in [6].

4 Breakup Models

4.1 Introduction

The breakup models discussed in this section are the theoretical models that describe the breakup of the droplets in the secondary breakup. By diving deeper into the physical meaning of the different models a good understanding can be formed which helps in reasoning which model is likely to produce proper results in the end. The different models are also compared, this is essential, because the goal of this paper is to recommend which model gives the most reliable results.

4.2 Taylor-Analogy-Breakup

The Taylor analogy Breakup, shortened as TAB, is the first method to be considered for the use of modelling the secondary Breakup. This model was proposed by O'Rourke and Amsden in 1987 [7] and is based on an analogy by Taylor [8]. The TAB analogy models a droplet as a mass-spring-damper system, where the spring force, external force and dampening are in terms of the droplet represented by the surface tension, aerodynamic forces and drop viscosity, respectively [9]. This relation can be described as is done in Equation 4.1

$$m\ddot{x} = F - kx - d\dot{x} \tag{4.1}$$

with m the droplet mass, F the (aerodynamic) force, k the spring constant and d the damping constant.

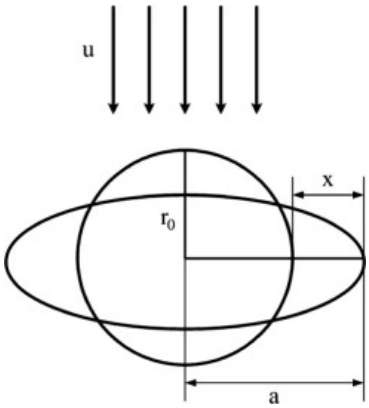

Figure 4.1: Schematic Representation of a droplet and its deformation according to the TAB model [9]

.

In the second order equation the value x represents the deviation of the distorted form of the droplet compared to its equilibrium, also visualized as the x in Figure 4.1. The variable a in Figure 4.1 is the radius of the distorted droplet and r_0 the original radius of the droplet.

An important criterion that needs to hold for y in Equation 4.1 is that y<1 for the breakup to occur, according to O'Rourke and Amsden [7]. The value y in the above equation represents the ratio between the distorted radius and the original radius of the droplet, which is then multiplied with a constant C_b being equal to $\frac{1}{2}$. This relation is shown in Equation 4.2.

$$y = \frac{a}{C_b r_0} \tag{4.2}$$

The physical meaning for each of the coefficients in Equation 4.1 can be expressed in the following formulas;

$$\frac{F}{m} = C_F \frac{\rho_g U^2}{\rho_l r_o} \tag{4.3}$$

with C_f the dimensionless coefficient for the force.

$$\frac{k}{m} = C_k \frac{\sigma}{\rho_l r_o^3} \tag{4.4}$$

with C_f the dimensionless coefficient for the stiffness.

$$\frac{d}{m} = C_d \frac{\eta_l}{\rho_l r_o^2} \tag{4.5}$$

with C_d the dimensionless coefficient for the damping.

The dimensionless constants C_F, C_k and C_d are 8, $\frac{1}{3}$ and 5 respectively. Substituting Equations 4.3, 4.4 and 4.5 into Equation 4.1 gives the following relation for the oscillation of the drop surface with having $y = \frac{x}{C_b r}$. The formula for y represents the ratio between the distorted radius and the original radius of the droplet, which is multiplied with a factor C_b, where C_b equals $\frac{1}{2}$. According the O'Rourke and Amsden [7] breakup only occurs if y > 1. All the dimensionless coefficients that are shown in this section are determined by comparing experimental and theoretical results performed by O'Rourke and Amsden [7].

$$\ddot{y} = C_F \frac{\rho_g u^2}{\rho_l r_o^2} - C_k \frac{\sigma}{\rho_l r_o^3} y - C_d \frac{\mu_l}{\rho_l r_o^2} \dot{y} \tag{4.6}$$

The TAB method works better in the bag break-up, which occurs in a range of 12 < We <40-100, as stated in [10], [11]. The TAB model is an often used, well defined and robust model when it comes to breakup modelling. Therefore, the TAB model is a good candidate for modelling the secondary breakup.

4.3 Kelvin–Helmholtz Instability

The Kelvin-Helmholtz instability is the second method that is considered for simulating the breakup. The KH-Instability is different than the TAB method in terms of which perspectiveis used for modelling the droplet. For KH, instability occurs when velocity shear is present in a single continuous fluid or a velocity difference in the boundary of two flowing fluids. In gas atomization, velocity shear is present in the incoming gas stream and injected fluid. Further, KH models the breakup as disturbances growing on the droplet surface, while TAB uses a second order differential equation.

In general the Kelvin-Helmholtz instability is in line with experimental data for the Weber number in the range 80 < We < 800 [10]. For this range of Weber numbers the way of droplet atomization is sheet stripping, as is shown in Figure 3.1, and for We > 350 the catastrophic breakup occurs.

The criterion where the KH-Instability focuses on is the fastest growing disturbance on the surface of the droplet. The fastest growing disturbance is likely to cause the breakup of the droplet, the corresponding wavelength can be described by Equation 4.7.

$$\Lambda = \frac{9.02(1 + 0.45Z^{0.5})(1 + 0.4T^{0.7}))}{(1 + 0.87We_{gas}^{1.67})^{0.6}} r \tag{4.7}$$

In Equation 4.7 the Z and T term come down respectively to the following equations:

$$Z = \frac{We_{liquid}^{0.5}}{Re} \tag{4.8}$$

$$T = ZWe_{gas}^{0.5} \tag{4.9}$$

The Weber numbers used in the above equations are the individual Weber numbers for both the liquid and gas.

$$We_{liquid} = \frac{\rho_{liquid} U^2 r}{\sigma} \tag{4.10}$$

$$We_{gas} = \frac{\rho_{gas} U^2 r}{\sigma} \tag{4.11}$$

The Reynolds number used in the KH-Instability is the Reynolds number from the liquid and is formulated by:

$$Re = \frac{\rho_{liquid} U d_p}{\eta_{liquid}} \tag{4.12}$$

The growth rate of this particular wavelength can be described by Ω. The growth rate gives an indication of the speed of the growing wavelength. The formula for this growth rate is described with Equation 4.13.

$$\Omega = \frac{0.34 + 0.38We_2^{1.5}}{(1+Z)(1+1.4T^{0.6})} \sqrt{\frac{\sigma}{\rho_l r^3}} \tag{4.13}$$

If the growing disturbance becomes large enough the droplet causes the breakup.In the KH-instability this breakup is modeled as small droplets are formed from parts of the parent droplet. The radius of the new droplet resulting from this breakup is proportional to the wavelength of the largest growing unstable wave.

$$r = B_0 \Lambda \tag{4.14}$$

B_0 in Equation 4.14 is a model constant which is equal to 0.6 [6], [7].

The time it takes for the droplet to breakup can be described with Equation 4.15

$$t_b = \frac{3.726 B_1 r}{\Omega \Lambda} \tag{4.15}$$

with B_1 being an adjustable constant that differs depending on which breakup regime is present.

The Kelvin-Helmholtz instability can be a suited method to model the secondary breakup. Because, in the secondary breakup a large velocity difference between the droplets and the inflow of the gas is present. Also, the range of Weber numbers wherein the KH-Instability is shown to work well, is convenient since it is also the range of Weber numbers where the simulation will be present.

4.4 Comparison

In this section the different mathematical models, discussed above, are evaluated and compared. The main difference between the models is the fact that the Taylor analogy breakup models the breakup as a second order differential equation perspective. Whereas the Kelvin-Helmholtz models the breakup from a disturbance/wavelength point of view.

The TAB method seems to work better in 12<We<40-100. The KH-Instability performs best in a range of 80¡We¡800. In Table 5.1 the Weber number can be seen for different type of cases where the air stream velocity is varied per case. This means that the TAB is most likely to perform well in the cases with a low air stream velocity as in Case 2 and 3. The KH-Instability tends to work better in a range of higher Weber numbers than the TAB-method and therefore is expected to perform well from case 4 to 9.

The result of this thesis is which model is the most accurate and is investigated in the next chapters where the data from the paper by Liu et al. is compared to the obtained simulation data in openFoam.

5 Benz Breakup

This section describes the paper that is used for evaluating the different models and the way of working from the researchers. The motivation of choosing the work from Liu et al. is that they described their way of working in both the experiments and simulations in a clear way. The paper is reproducible, which is important for creating a validation case.

The implementation of the exact same paper in the CFD software openFoam is described. Subsequently, the results of the openFoam implementation are compared and evaluated with the results originating from the paper [6]. Firstly, the single droplet breakup is compared and after that the breakup for a stream of droplets.

5.1 Reproducing Existing Experiment and Simulation

In order to evaluate the used models, simulations are carried out to validate the implemented breakup models in openFoam. This is done by reproducing the experiment from Liu et al. [6]. In this paper an experiment is executed and subsequently models are used to simulate the experiment in a numerical way and each model is compared to the experimental data for an evaluation on their performance. The models that Liu et al. have just in their work are both the TAB and KH models. The data that can be compared consists out the trajectories, drop sizes of single droplets and Sauter mean diameters.

The droplets were injected into a relatively high velocity gas flow. The paper from Liu et al. is based on the breakup of fuel sprays instead of molten metal, which is eventually the goal. By reproducing the experimental results from the paper [6] a validation of the models can be performed. In this way, the TAB and KH models, can be compared to the accuracy of modelling the secondary breakup. Models that succeed in reproducing the experimental data can be considered as useful for modelling the secondary breakup for diesel applications. Subsequently, predictions can be drawn on how the models will behave when molten metal is the fluid.

5.2 Experiment

The performed experiment from the paper is described in this section. Important parameters and properties are discussed and the results found by Liu et al. are evaluated.

5.3 Setup

The experiments performed by Liu et al. consisted out of a drop generator and an air nozzle. A monodisperse stream of liquid drops was generated and injected into the air stream. The diameter of the drops at injection was 170 μm and had a horizontal velocity of 16 m/s. The droplets were injected 2 mm at the edge of the air stream nozzle. The way of injecting is schematically visualised in Figure 5.1. In this figure there can be seen that the droplets are injected on the left side of the air stream and the air stream is flowing downwards.

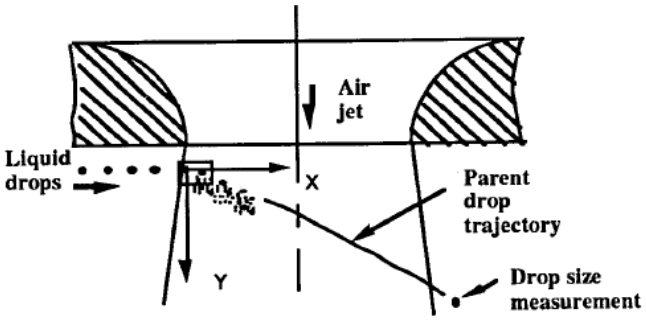

Figure 5.1: Schematic overview of the experimental setup.

However, the injection location is described by Liu et al. it can still be interpreted in two ways. As the edge of the air stream can be the most outer edge of the nozzle diameter or where the vertical velocity equals zero.

The inlet nozzle had a diameter of 9.525 mm and the air jet resulting from the air nozzle had a velocity that was varied between 0 and 250 $\frac{m}{s}$. The axial velocity had a flat profile at the injection location. Each of the cases can be seen in Table 5.1. The experiments were performed under atmospheric pressure and room temperature.

Case	Air Velocity [m/s]	Weber	Reynolds	Breakup Regime
1	0	0	0	-
2	59	36	669	bag
3	72	53	816	bag
4	100	102	1133	bag
5	136	189	1541	stripping
6	152	236	1723	stripping
7	188	361	2131	surface wave
8	214	467	2425	surface wave
9	250	638	2833	surface wave

Table 5.1: Case data used by Liu et al. [6]

The liquid they used in the experimental breakup was Benz UCF-I test fuel, as the goal for the researches was to model the breakup for diesel applications. The properties of the Benz UCF-I can be seen in Table 5.2.

Benz UCF-I	Density [kg/m^3]	Dynamic viscosity [Pas]	Surface Tension [kg/s^2]
	824	2.17e^{-3}	2e^{-2}

Table 5.2: Properties of Benz UCF-I used in experiments and simulations.

5.4 Measurements

Extracting data out of the experiments is crucial for the comparison and evaluation between the models. At low velocities the parental droplet could be measured at the moment when it entered the other side of the air stream. The diameter is measured with the aid of an Aerometrics phase/Doppler particle analyzer. However, at higher velocities of the gas stream,

droplets remained inside the stream or the resulting droplets were too small to measure them properly, according to [6]. Therefore, this way of measuring has only been applicable to Cases 2&3, which can be seen in Table 5.1.

The trajectory of the droplets have been measured by photographs that are taken during the breakup. Liu et al. described that the measurements relies on the knowledge that the side of the air stream is known in order to have a reference location for starting the trajectory. They stated that the edge of the air jet is known with an accuracy of 0.25 mm.

5.5 Simulation

Liu et al. described their way of simulating and reproducing the experimental data. It is important to have the exact same mesh sizes and flow conditions in order to be able to reproduce the experimental/numerical data provided by [6] in a valid way.

5.5.1 Mesh

The mesh used in the simulation is a cylindrical domain. The diameter of the cylinder equals 52 mm and the height 57 mm. The amount of cells in each direction is respectively specified as 32x16x84 cells in the radial, azimuthal and axial. This comes down to a total amount of 43.008 cells.

The mesh described in the paper is created in openFoam by using blockMesh. This mesh can be seen in Figure 5.2a.

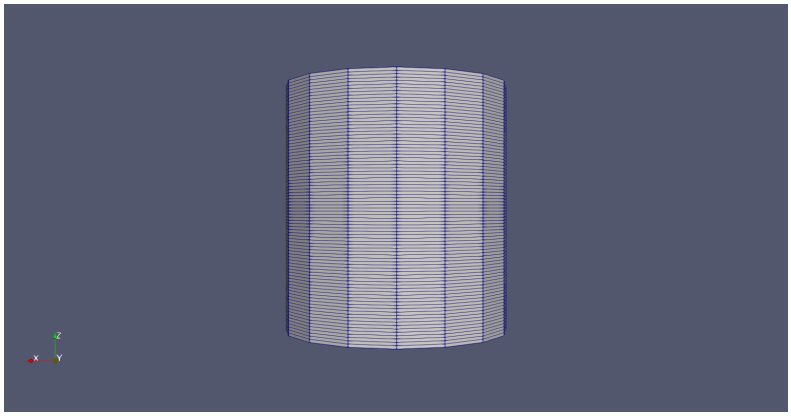

(a) Front view of the cylindrical mesh recreated with blockMesh in the software Openfoam.

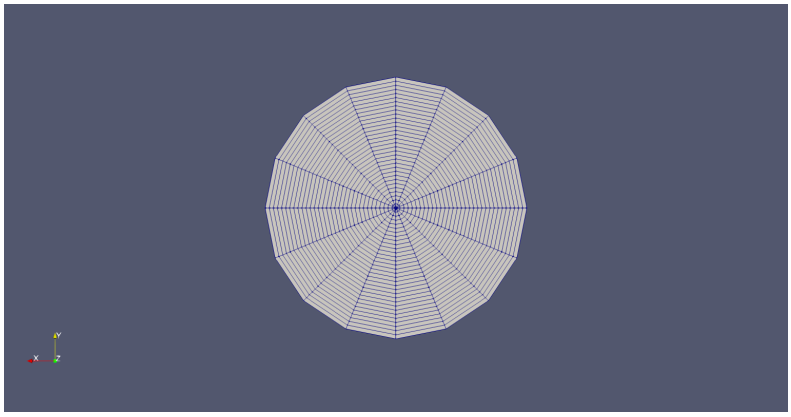

(b) Top view of the cylindrical mesh recreated with blockMesh in the software Openfoam.

The generated mesh is divided into different patches. It is important to have the right patches inside the mesh. In this case, the patches are the inlet, walls and outlet. For the the different patches specific boundary conditions are applied for recreating the simulation in a proper way.

The inlet in the mesh is the same as the air nozzle described in the paper. The air nozzle is a circular patch in the top of the domain with its origin in the center. The diameter of the air nozzle is 9.525 mm.

5.5.2 Flow conditions

During the simulation and experiment a constant air stream is flowing out of the inlet. For reaching the velocity of each of the cases presented in the paper by Liu et al. A gradual increase per timestep is implemented in order to have a simulation without any continuity errors. The gradual increase is implemented by using #codeStream inside openFoam, which allows time and location dependant coding of initial -and boundary conditions. In Figure 5.3 a visualization of the inflowing air stream is shown.

The droplets are inserted with an initial velocity of 16 m/s. The injection location is at the edge of the velocity stream and 2 mm below the inlet nozzle. This is the same injection as is used in both the experiments and simulations described by Liu et al.

The location of the droplet can be seen in the figure below. The droplet is shown in white and is visible on the left edge of the nozzle. The droplet is injected as the velocity field is fully developed. In this case this means that a continuous flow of 59 m/s needs to be reached.

Figure 5.3: Visualization of the inflowing air stream and the injection location of the droplets for case 2

Now the simulation setup is specified and explained. The next sections will show results from the data presented by Liu et al. and simulations from current work.

6 Single Droplet Breakup

6.0.1 Results Liu et al.

The results of the simulations are evaluated with the data presented in the paper of Liu et al. First, they show their results of a single droplet interacting with the inflow air stream. In these plots, Case 4 is simulated with the Wave breakup model using a factor $B1 = 1.73$. The factor $B1$ is the time constant for the characteristic breakup time, as is shown in Equation 4.15. $B1 = 1.73$ has been used for every simulation that follows, since Liu et al. showed good agreement on experimental data [6].

The Reynolds number and parent drop diameter are evaluated over the horizontal penetration distance into the air stream. The results for the Reynolds number and droplet diameter are respectively visualized in Figure 6.1a and Figure 6.1b.

Below an explanation of the results obtained from Liu et al. is given and thereafter the results of the current work simulation are evaluated.

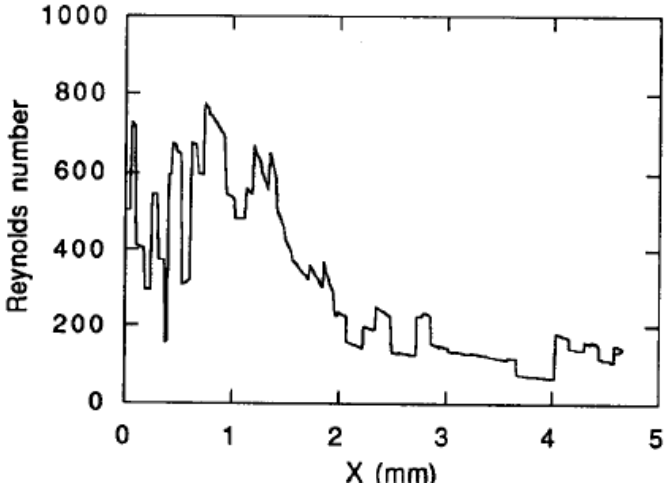

(a) The Reynolds number over the horizontal penetration distance for Case 4. [6]

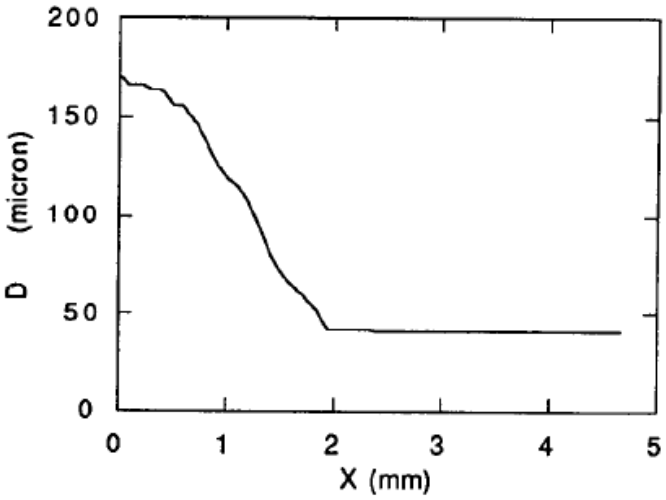

(b) The parental droplet diameter over the horizontal penetration distance for Case 4. [6]

In the results of Figure 6.1a, an immediate rapid peak can be seen in the behaviour of Re. This peak starts as soon as the droplet is injected at the edge of the air stream. This is a result of the sudden change in velocity due to the interaction of the air stream. As the droplet travels further through the air stream the Reynolds gradually decreases. Liu et al. describe the fluctuations in the Reynolds number to be due to the gas turbulence.

For the parental droplet diameter a continuous decrease is present as soon as the drop travels through the air stream. The decrease in diameter ceases as the droplet has travelled 2 mm through the air stream. Due to the decrease in droplet diameter, which is in the numerator of Equation 3.1, results in turn into a smaller Weber number. If the diameter is decreased to a point that the Weber number is below the critical Weber number. Breakup does not occur and therefore the diameter remains constant after the 2 mm.

6.0.2 Results current work

The single droplet breakup of case 4 is modelled in openFoam and the same parameters as in the paper are implemented. The results of the simulation are compared in this section with the results from the paper.

In order to create a good comparison between the data from the paper and the openFoam simulations the graphs from the paper are recreated. Both the recreated data from the paper and the results of the performed simulation are visualized in the figures below. Important to note is that the horizontal penetration distance plotted in the figures below is from a range -4.7625 mm and further. This is done as the injection location in the simulation of current work is also exactly -4.7625 mm.

The original Reynolds number and droplet diameter from the paper are shown by the orange dashed lines in Figure 6.2 and Figure 6.3. The results from the current work are plotted in the same graphs, this can be seen in the figures 6.2 and 6.3 as the blue line.

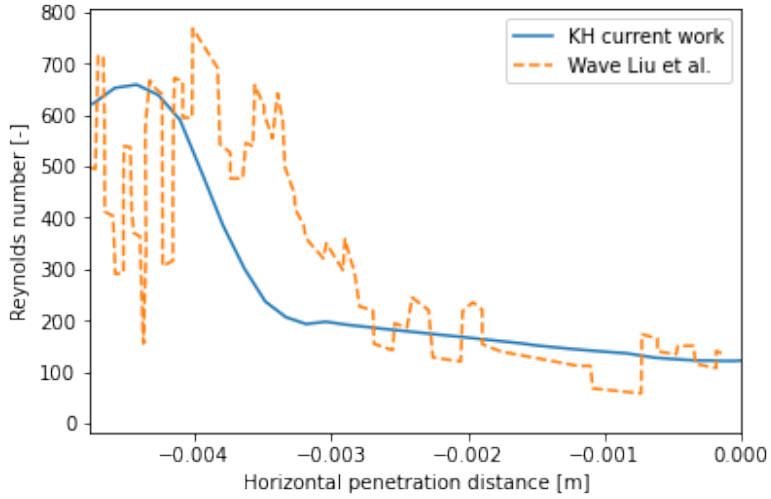

Figure 6.2: The Reynolds number over the horizontal penetration distance for Case 4.

There can immediately be seen that the data from the paper about the Reynolds number contains much more deviations than the data from the simulations. However, the overall behaviour of the Reynolds number is the same throughout the whole horizontal penetration distance, except for the fact that the droplet from current work reaches its maximum Reynolds number sooner than the data from Liu et al.

The large Reynolds number at the start of the droplets trajectory is caused by the fact that the drop just has entered the air stream. The Reynolds number increases significantly due to the increase in relative velocity between the droplet and its surrounding.

The maximum in Re is followed by a large decrease. This is caused by the breakup of the droplet, because the Reynolds number decreases with a decreasing droplet diameter as can be seen in Equation 3.3. The decrease in diameter comes to a halt sooner than the data from Liu et al. although this is present with the same shift.

After the droplets breakup a slight decrease in Re is present. This effect is caused by the fact that the droplet increases in velocity as it travels further downstream. Therefore, the relative velocity decreases and since Re is proportional to the relative velocity it decreases as well.

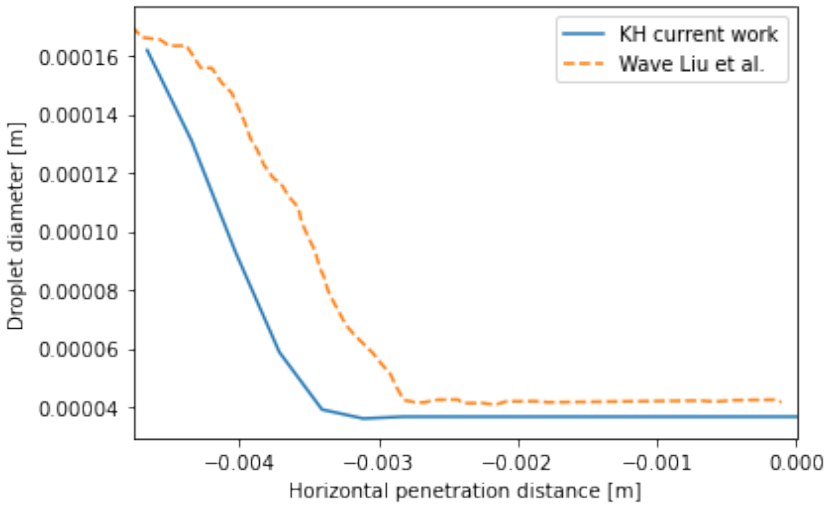

Figure 6.3: The parental droplet diameter over the horizontal penetration distance for Case 4.

The behaviour of the droplet diameter over the horizontal penetration distance can be seen in Figure 6.3. A first observation is that the overall behaviour throughout the droplets trajectory compares well with the reference data from the paper. Again, the breakup starts sooner than there is presented by Liu et al. Despite the earlier start of the breakup the slope of the breakup is equal to the slope of the reference data. In the end the final droplet diameter converges to almost the same diameter. Simulations with an injection location at the edge of the velocity field instead of the nozzle show better alignment with the reference data. However, the implemented KH-model did not always give reliable diameters for those simulations therefore the edge of the nozzle is chosen for the simulation to follow.

In both results a large decrease can be observed in the diameter as the droplet enters the air stream. Although, the decrease does not stop at the exact same horizontal penetration distance, it does stop at the same droplet diameter which is in current work 40 μm and from Liu et al. just above the 40 μm. After the breakup has stopped the diameter does not decrease anymore. In terms of the KH-instability this means that the growing disturbance and the critical diameter is not reached, which does not result in breakup. This is proportional to the Weber number of the liquid as is shown in Equation 4.7 and Equation 4.13.

The behaviour of the Reynolds number is similar to the Weber number. As the droplet diameter decreases due to the breakup there is a decrease in Weber number as well. Therefore, the growing disturbance decreases and does not exceed the droplet diameter itself, which results in no breakup anymore.

For the single droplet breakup modelled by using the KH-Instability there is shown that except for the start of the breakup the results from current work are in line with the results presented by Liu et al. The Reynolds number shows the same behaviour, however without less deviations. The droplet diameter shows a clear in line behaviour with the data from the paper except for the start of the breakup.

Next, the single droplet breakup is compared and shown that the results of the KH-model correspond with each other, further simulations are done where compare the Sauter mean diameter and droplets trajectory as a function of the horizontal penetration distance are compared. For the following simulations averages are taken of multiple droplets as Liu et al. also described in their case. The graphs from Liu et al. are for each case recreated and simultaneously shown with the results from current work.

7 Sauter Mean Diameter

First the sauter mean diameter from current work is compared with results from the paper. Liu et al. presented data for the SMD for the cases 2 & 3. These cases were the only cases where data from the experiments could be obtained by the PDPA. Only in these two cases droplets reached the other side of the air stream.

7.1 Case 2

Case 2 is the first case that is evaluated. Firstly, the results from Liu et al. are compared with the experimental data. After that, each model is compared with the paper and the experimental results.

7.1.1 KH

In Figure 7.1 the results of the simulations using the KH-models of the current work, the paper and the experiment are visualized. The figure shows that the data from Liu et al. contains a decrease in diameter as soon as the droplet is injected into the air stream. This is caused by the abrupt increase in relative velocity to which Re is proportional. The decrease in diameter ceases gradually. Comparing the simulation from Liu et al. with the experiment shows that the SMD outside the air stream comes close to the experimental data.

The results from current work show that the droplet breakup starts earlier than the results from the paper. This exact same behaviour is observed in the single droplet case from previous chapter. The decrease in SMD also ceases sooner in comparison with the paper. That the SMD converges earlier for current work might be caused by the rate of breakup over the horizontal position. The rate of breakup is the slope of the decrease in SMD. This rate is larger in current work.

The rate is described by Equation 4.14 and is inversely proportional to the fastest growing wavelength and its corresponding growth rate. Although, this rate is modelled with the same breakup time constant $B1$ it seems to differ in current work. Another cause can be the uncertainty about the injection location as is described earlier in this thesis.

The final SMD of the droplet when it escapes the air stream is completely in line with the results from Liu et al. Both diameters converge to same end diameter, which gives confidence in the results of the final SMD outside the air stream in current work.

Because of the same behaviour in end diameter the results from current work perform the same in comparison with the PDPA measurement. Although, the final Sauter mean diameter is not exactly the same with the measurement. The results come close and both models converge to the same result.

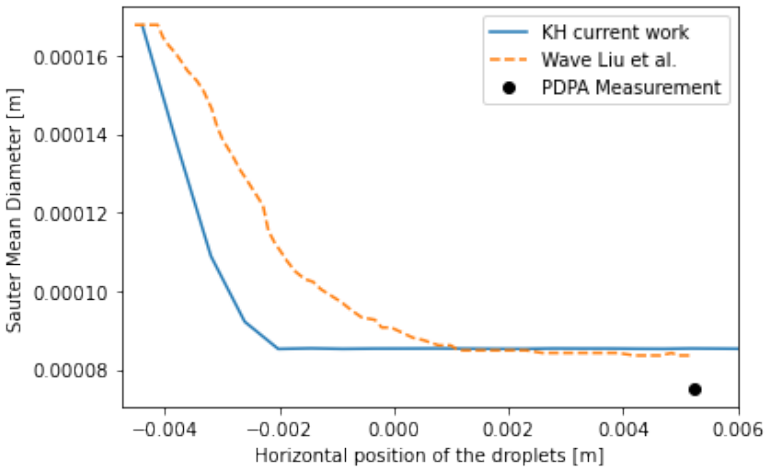

Figure 7.1: Sauter mean diameter results from the KH-model for current work and reference data in case 2

7.1.2 TAB

Figure 7.2 shows the data for the TAB simulations and the experiment. The results from Liu et al. show that the TAB model do not have an immediate breakup as it has entered the air stream, it takes a certain distance to start. It is important to recall that breakup only occurs if the ratio between the distorted droplet radius and the original radius is larger than 1, seen in Equation 4.2.

If the distortion parameter y is larger than 1, there can be seen that the breakup occurs more abrupt as the SMD decreases with a steep slope. Finally, it converges to a SMD below 60 μm. Comparing their model to the PDPA measurement there can be concluded that the TAB model overestimates the droplet breakup as it results in a significant smaller diameter.

Similar behaviour in current work is observed in the breakup of the droplet. The constant diameter in the first horizontal movement of the droplet is less present, which means that the TAB model in current work reaches the $y > 1$ constraint sooner. However, the steep slope in decrease of the SMD behaves similarly with the results from Liu et al. In the TAB simulations from current work, the breakup starts sooner in comparison with the reference data, just as it is observed in the KH-model.

The SMD at the end of the air stream equals the SMD from Liu et al. This shows that the TAB model seems to overestimate the breakup in both the current and the reference data.

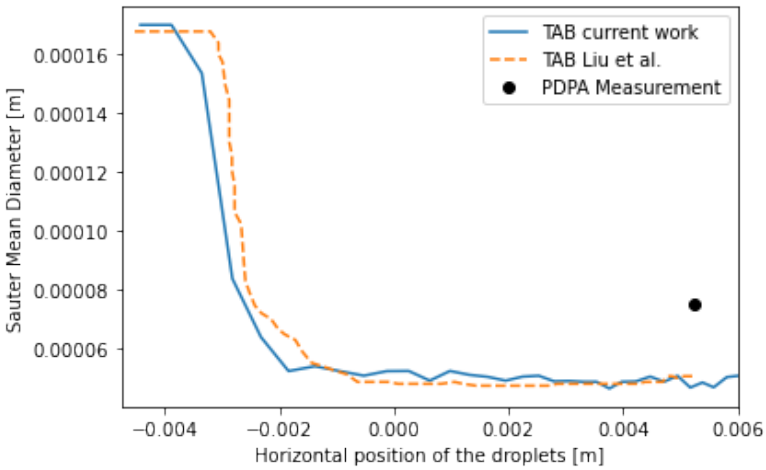

Figure 7.2: Sauter mean diameter results from the TAB-model for current work and reference data in case 2

7.2 Case 3

Case 3 is the second case where SMD data is present from the experiment. The results from current work and work from the paper are compared and discussed.

7.2.1 KH

Figure 7.3 shows the results from current work, Liu et al. and the experiment. The droplets have an immediate breakup just as is presented in Figure 7.1. The droplets are decreasing gradually until the droplet becomes stable and the largest disturbance wavelength can not cause the droplet to breakup. Comparing the results from Liu et al. with the PDPA measurement there can be seen that the PDPA measurement turns out to be lower than simulations show.

The KH-model used in current work shows a breakup that again starts sooner. The slope of the decrease seems to be in line with the reference data. In results from current work the transition between breakup or no breakup seems to be more abrupt, however this can be caused by a smaller amount of sampling data from the simulations.

The final SMD of current work is lower than the SMD from Liu et al. Current work shows that the SMD converges to a SMD that is closer to the reference data from the experiment.

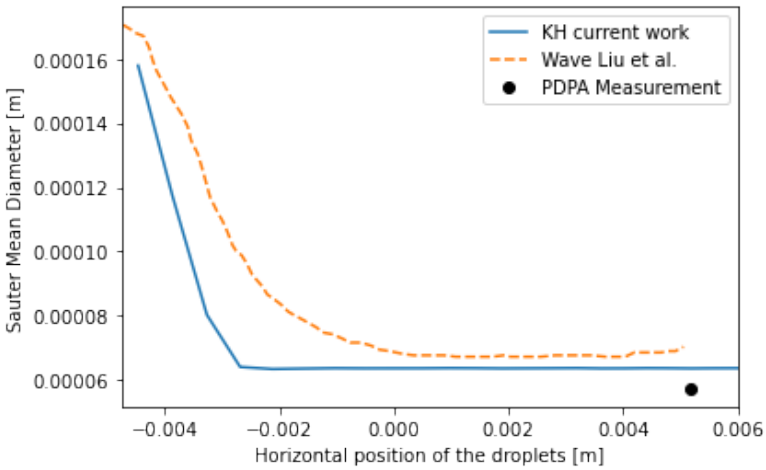

Figure 7.3: Sauter mean diameter results from the KH-model for current work and reference data in case 3

7.2.2 TAB

The TAB model from the paper shows a constant SMD at the horizontal movement of the droplets when they just have entered the air stream. The decrease in SMD is in case 3 also steep and ceases until the drop distortion parameter y does not exceed one anymore. Results from Liu et al. come close to the PDPA measurement, but still show a difference between what is measured and simulated.

The TAB model used in current work tracks the same behaviour as the reference data. The start of breakup is at the same horizontal movement. Also, the diameter after the breakup shows a match with the reference data.

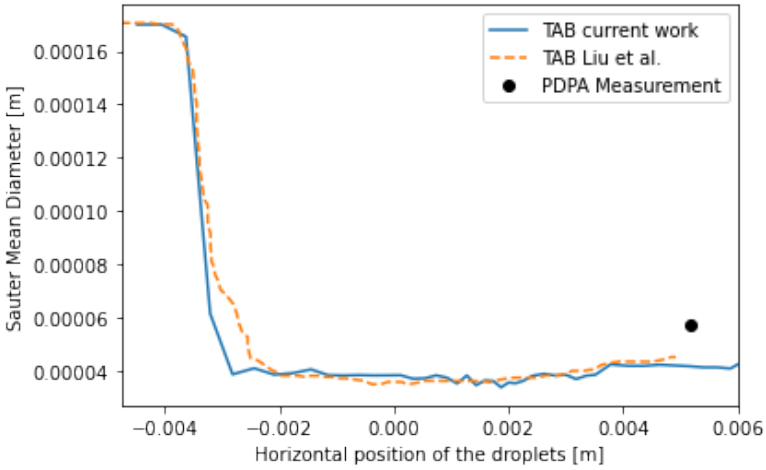

Figure 7.4: Sauter mean diameter results from the KH-model for current work and reference data in case 3

In general there holds for the Sauter mean diameter that the KH-model starts sooner with the breakup than the reference data. The earlier breakup can be caused by a difference in the rate of breakup, which is faster in current work. The difference can be caused by a mediocre change in the code used in openFoam and Liu et al. as the code also makes used of if-constraints where the Weber number is involved which is not the case in the paper. The TAB model tracks the reference data well, however in case 3 better than in case 2.

8 Trajectories

Besides the SMD, the droplet trajectory is an important result for the breakup. Simulations are carried out for the cases that Liu et al. presented in their paper. The results of current work and their data is compared and evaluated in this section.

8.1 Case 2

In case 2 the air stream velocity equals 59 m/s. This is the case with the lowest air stream velocity and therefore shows the least deflected trajectory. First the KH-model is compared to the similar wave model from Liu et al. Subsequently, a comparison is made for the TAB model.

8.1.1 KH

In Figure 8.1 the current work and results from Liu et al. are visualized. The simulation from the paper tracks the experimental data well.

Comparing current work with the experimental data and their simulation, there can be observed that current work is not in line with the reference data. The trajectory is less deflected. In Figure 7.1, there is shown that for current work the breakup starts sooner. An earlier breakup also means a smaller SMD at a lower horizontal position. Therefore, one would expect a more deflected trajectory than there is presented by Liu et al.

This is certainly not the case and therefore the trajectory results from the current work do not align with the results from Liu et al.

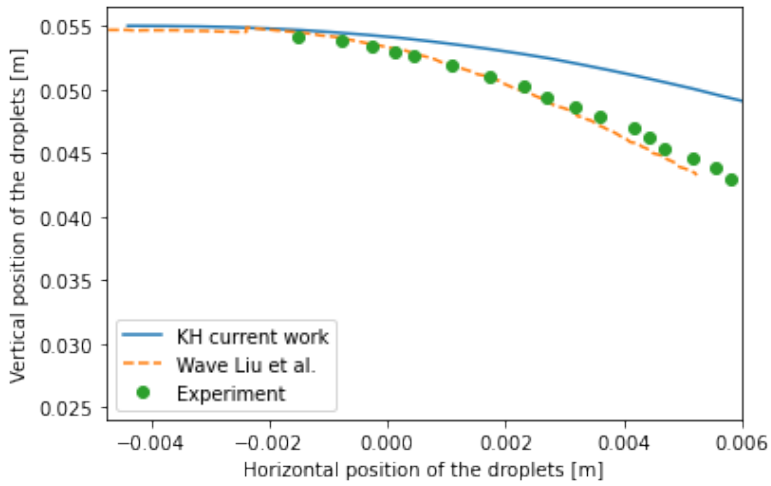

Figure 8.1: Trajectory results from the KH-model for current work and reference data in case 2

8.1.2 TAB

The results from Liu et al. show that the experimental data is tracked well. Results from the current work shows that the trajectory is not in line with the reference data.

The behaviour of the SMD for the TAB model of current work in Figure 7.2 shows that the breakup starts sooner, which results in a smaller diameter at a smaller horizontal position. A smaller diameter means a smaller mass of the droplet. Having a smaller mass early in the breakup causes a more deflected trajectory, since less energy is necessary for deflecting the droplet. This can cause the more deflected trajectory in the TAB model in current work.

From a horizontal position of 4 mm deviations in the trajectory are noticeably present. These deviations are due to the limited simulation data from simulations in current work.

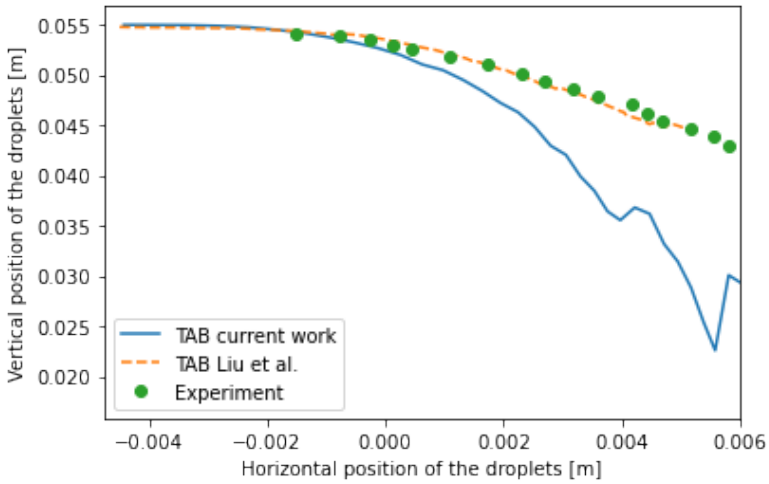

Figure 8.2: Trajectory results from the KH-model for current work and reference data in case 2

8.2 Case 4

Case 4 is the second case from which the trajectories can be compared between current work and the results from Liu et al. The results are compared and evaluated below.

8.2.1 KH

The results from the paper are tracking the experimental data well. In comparison with case 2, the trajectory differs more. Data from current work show a less deflected trajectory. There is no SMD data available for case 4, but looking at Figure 7.1 and Figure 7.3 the behaviour of these two is the same. In both cases the breakup occurs sooner than the breakup in the reference data. Therefore, in case 4 a more deflected trajectory is again expected to be observed.

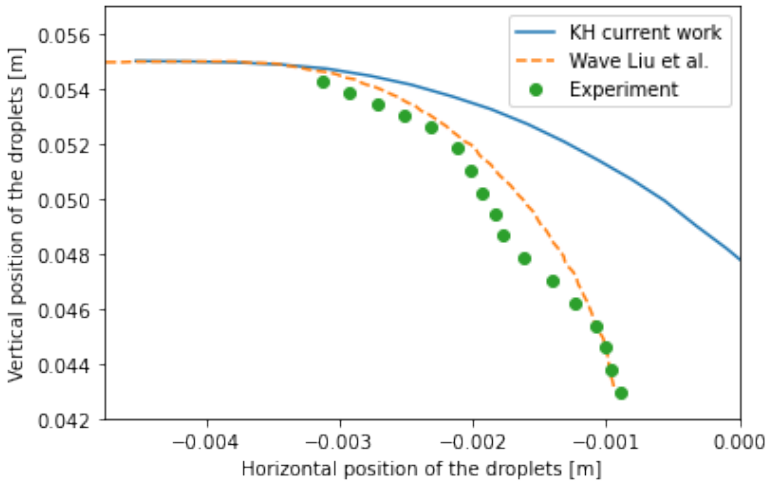

Figure 8.3: Trajectory results from the KH-model for current work and reference data in case 4

8.2.2 TAB

In Figure 8.4, the trajectory of the TAB models for case 4 are visualized. The data from Liu et al. show clear tracking of the experimental data. Results from current work show a larger deflection in trajectory in comparison with both the simulation and experimental data.

The heavier deflection presented in this case can not be directly linked to the behaviour of the decrease in SMD. Although, case 4 does not have reference data for the SMD. By looking at the behaviour of the decrease in SMD from Figure 7.2 and Figure 7.4, the reason for a more deflected trajectory can be caused by the fact that the TAB model in general overestimates the breakup.

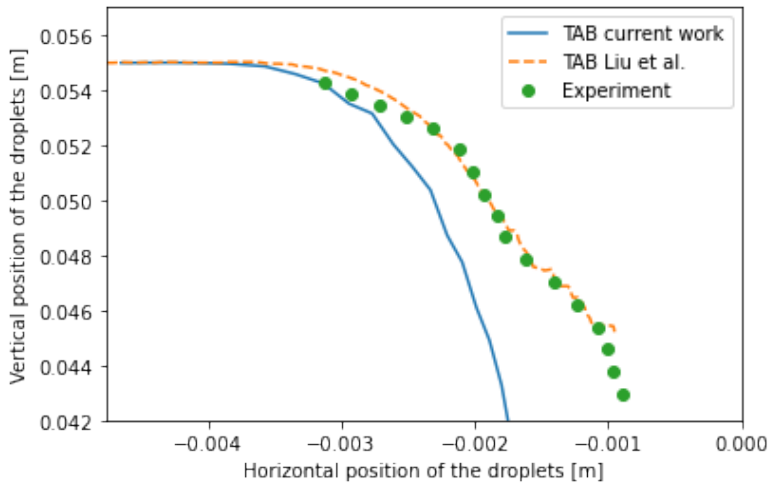

Figure 8.4: Trajectory results from the TAB-model for current work and reference data in case 4

In general there is a clear line in the behaviour of the models from current work. The KH-model underestimates the droplet breakup, whereas the TAB model overestimates the droplet breakup. This is neither the case for the data presented by Liu et al.

8.3 Model Comparison

The result of this thesis is an recommendation on which model gives reliable and correct results. Now the individual results of the models have been compared with the reference data. It is of utmost importance to compare both models from current work between each other.

8.3.1 Sauter mean diameter

The comparison is done in this section for the Sauter mean diameter. Figure 8.5a and Figure 8.5b plot the current work with the experimental data for case 2 and case 3, respectively.

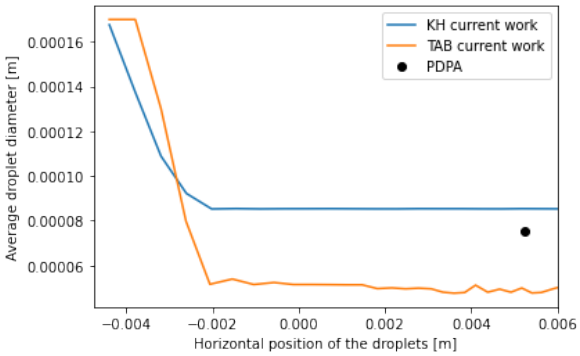

(a) Sauter mean diameter for the KH-model from current work for case 2

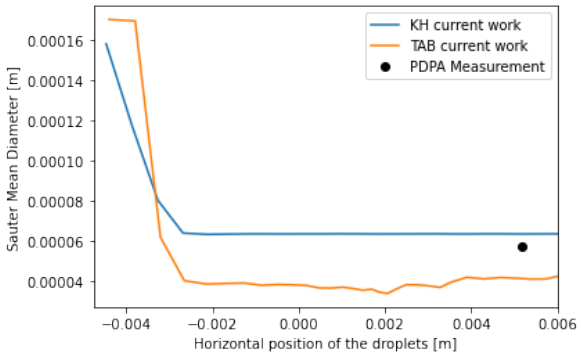

(b) Sauter mean diameter for the KH-model from current work for case 3

The behaviour of the two models differs significantly. The KH-model has a gradual decrease in SMD as the droplet has entered the air stream in both cases. In contrary, the TAB model shows at first a constant SMD, until the drop distortion parameter exceeds one. The breakup for the KH-model seems to ease more out into the final diameter than the TAB-model. When the breakup has ceased both models result in a constant SMD.

The difference in the final SMD is due to the fact that the KH-model gradually decreases the parental droplet based on the breakup time and the radius of the child droplet respectively from Equation 4.15 & Equation 4.14. This gradual decrease is also visible in the figures above.

In the TAB model, the parental droplet completely breaks up into child droplets when $y > 1$ and therefore there is no surviving parent droplet in the TAB-model. This abrupt breakup of the parental droplet also explains the steep slope present in both cases for the TAB-model.

The final SMD outside the air stream is the point that can be compared with the PDPA measurement. The KH-model shows in both cases better agreement to the final SMD than the TAB-model and therefore is from a SMD point of view more in line with the experimental data.

8.4 Trajectories

The trajectories from current work did not align well with the simulations presented by Liu et al. In this section the comparison between the two models and the experimental data is done.

In Figure 8.6a and Figure 8.6b the comparison between the models is plotted for respectively case 2 and 4. In both graphs the KH-model seems to underestimate the deflection of the droplet during breakup, whereas the TAB model seems to overestimate it in comparison with the experimental data.

The graphs from Figure 8.5a and Figure 8.5b clearly show that the diameter is not the same for the two breakup models. The KH converges to a larger SMD than the TAB model. This results in a difference in trajectory. As the mass of the droplet is proportional to the diameter of the droplet. A larger diameter means a larger mass. Subsequently, a larger mass means more momentum as the droplet is moving, which requires more energy to deflect the trajectory of the droplet. In this case, the KH-model would require more energy and this would show in a less deflected trajectory in comparison with the TAB-model. Therefore, the results visible in the graphs are what is expected to happen. However, none of the used models is matching the experimental data. Therefore, the droplet trajectory on its own does not give information on which model performs better.

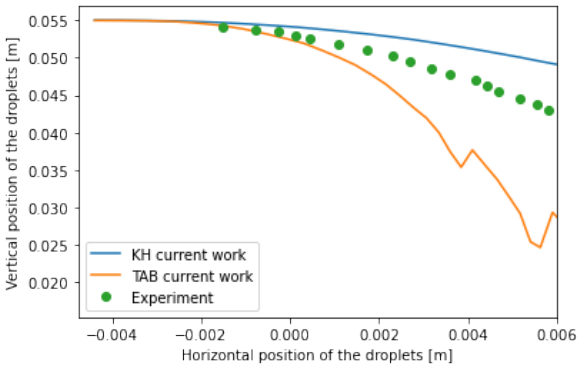

(a) Trajectory results for the KH-model from current work for case 2

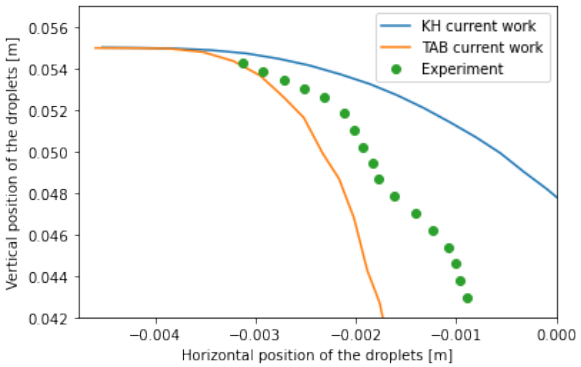

(b) Trajectory results for the KH-model from current work for case 4

9 Conclusion

The goal of this thesis is to give a recommendation on a model that is appropriate to use in modelling of the secondary breakup of metal gas atomisation. With a literature review possible suited models have been investigated on their way of modelling the breakup according to their formulas. Expectations were drawn with experience with these models presented in previous papers. The selected models from the literature research were the Taylor-analogy breakup and the Kelvin-Helmholtz methodology. A paper from Liu et al. also used these two models for the modelling the secondary breakup in Benz applications and presented their experiments and simulations. These simulations were recreated and carried out in the software openFoam. The results were compared and evaluated between the data presented by Liu et al.

The two models showed significant differences in the Sauter mean diameter. For the KH-model the breakup started sooner in both cases, comparison with the simulation from Liu et al. The breakup is dependant on the rate of breakup and the critical breakup size. The rate in current work uses the same breakup constant as is used in the paper. However, the model implemented in openFoam also uses additional conditions for breakup to occur than the KH-instability induces. This might cause the difference in breakup. Also, the injection location could be interpreted in two ways. Data has shown that an injection location at the edge of the velocity field is better in line with the reference data. This can also be the cause of the earlier breakup in the KH-model. Although, the start and rate differs from the simulation, the SMD to which the simulation converged is for both cases the same.

The TAB model shows for both the breakup and the Sauter mean diameter similar behaviour in comparison with the results from the paper. This gives confidence in the implemented TAB model.

The trajectories were for both models not in line with the presented data by Liu et al. The KH-model underestimated the droplets trajectory as it was not deflected as much as the experimental data or the simulation data. In contrary, the TAB model underestimated the droplet trajectory. As described in this thesis, the results obtained from the current work, is the result which is expected to happen. Namely, the difference in SMD between KH and TAB cause a difference in trajectory. This is because different sizes in droplets contain different masses, which results in different momentum. Since the air stream is the same for both models, there is also the same amount of energy that is able to deflect the droplets trajectory. Although, the behaviour of the models in current work is not matching the behaviour of the data from Liu et al. it is still what is expected to occur. Because of this, the trajectory is not a parameter to use on its own for confidently concluding which model performs better.

Now both models have been evaluated and compared extensively a final recommendation can be stated out of these results. The KH-model is in better agreement with the experimental data in comparison with the TAB model for the SMD. Moreover, knowing that the diameter is in the end a more important parameter than the trajectory of the droplet, since the interest lays in the resulting diameter. The KH-model is the final recommendation for using it in the secondary breakup.

10 Recommendations

The models that are used, show in general, a proper alignment with the reference data. There are still slight differences, which can be caused by mediocre changes in the code that is currently used in openFoam. Especially, for the KH model there are different if-statements than in the theoretical model. By having a more in depth look in the code it might be improved.

Another investigation can be performed on the TAB model by comparing the current model and the enhanced TAB model. This model is already present in openFoam. There can be investigated whether the enhanced TAB model indeed performs better by comparing it to the experimental data.

Turbulence modelling is an additional feature that can be added to the existing models. Since, there are high velocities present in gas atomisation turbulence can have an influence on the secondary breakup. Further research can be done on the effect of these models and their final results.

In this thesis there is shown that the models are in good agreement with the secondary breakup of the liquid Benz. However, in the end, the breakup models need to be applied to molten metal. Expectations can be drawn from current work, since important parameters for the liquid will change such as the density, surface tension and dynamic viscosity. However, they stay merely expectations and the result of this thesis can not confidently state whether this will be the real physical behaviour of molten metal. In the molten metal breakup, solidification is also present, this has not been modelled in this thesis. Therefore, it is recommended to investigate the performance of the KH-model on the secondary breakup of molten metal in a more extensive way and investigate models that take solidification into account.

References

[1] G. S. Antipas, "Liquid column deformation and particle size distribution in gas atomization," *International Journal of Computational Materials Science and Surface Engineering*, vol. 4, no. 2, pp. 87–96, 2011.

[2] M. Heinrich and R. Schwarze, "3d-coupling of volume-of-fluid and lagrangian particle tracking for spray atomization simulation in openfoam," jan 2020.

[3] H. Zhao and H. Liu, *Environmental Impact of Aviation and Sustainable Solutions*. IntechOpen, 2018.

[4] D. R. Guildenbecher, C. Lo´pez-Rivera, and P. E. Sojka, "Secondary atomization," *Experiments in Fluids*, vol. 46, no. 371, pp. 375–388, 2009.

[5] Z.Dai and G.M.Faeth, "Temporal properties of secondary drop breakup in the multimode breakup regime," *Experiments in Fluids*, vol. 27, no. 2, pp. 217–236, 2001.

[6] A. B. Liu, D. Mather, and R. D. Reitz, "Modelling the effects of drop drag and breakup on fuel sprays," 2019.

[7] O. PJ and A. AA, "The tab method for numerical calculation of spray droplet breakup," 1987.

[8] G. Taylor, *The shape and acceleration of a drop in a high-speed air stream*. Great Britain. Chemical Defence Experimental Establishment, 1963.

[9] M. W. Lee, J. J. Park, S. S.Yoon, and M. M. Farid, "Comparison and correction of the drop breakup models for stochastic dilute spray flow," *Applied Mathematical Modelling*, vol. 36, no. 9, pp. 4512–4520, 2012.

[10] N. Zeoli and S. Gu, "Numerical modelling of droplet break-up for gas atomisation," *Computational Materials Science*, vol. 38, no. 2, pp. 282–292, 2006.

[11] D. A. Firmansyah, R. Kaiser, R. Zahaf, Z. Coker, T.-Y. Choi, and D. Lee, "Numerical simulations of supersonic gas atomization of liquid metal droplets." Accessed: 2022-07-01.